Journal of Power Sources 225 (2013) 40–45

Contents lists available at SciVerse ScienceDirect

Journal of Power Sources

journal homepage: www.elsevier.com/locate/jpowsour

Short communication

The SEI layer formed on lithium metal in the presence of oxygen: A seldom considered component in the development of the Li–O_2 battery

Reza Younesi*, Maria Hahlin, Matthew Roberts, Kristina Edström

Department of Chemistry – Ångström Laboratory, Uppsala University, Box 538, SE-751 21 Uppsala, Sweden

HIGHLIGHTS

- The presence of O_2 influences the composition of the SEI on Li of the Li–O_2 battery.
- The SEI on Li anode of the Li–O_2 battery is unstable and changes during the cycling.
- $LiPF_6$ and PC decompose on the surface of the Li and contribute in formation of the SEI.
- Decomposed Kynar binder (degraded on the cathode) was observed on the surface of Li.
- Oxygen increases the resistance of the cells and influences the lithium stripping and plating.

ARTICLE INFO

Article history:
Received 4 July 2012
Received in revised form
24 August 2012
Accepted 8 October 2012
Available online 15 October 2012

Keywords:
Lithium-oxygen
Li-air battery
X-ray photoelectron spectroscopy (XPS)
Solid electrolyte interphase (SEI)
Lithium anode

ABSTRACT

The SEI layer formed on metallic Li which has been used as an anode in a Li–O_2 battery is studied for the first time. We have used XPS to monitor the surface composition of the lithium electrode and have identified the various chemical species present. The XPS results indicated that the composition of the SEI layer is affected by the presence of oxygen and is unstable during cycling. We also observed decomposition products from the binder material used in the cathode on the surface of the lithium anode. This new SEI layer has an increased resistance affecting the lithium deposition which is essential for battery operation.

1. Introduction

The demand for more advanced energy storage systems has grown in recent years and it is driven by the need for new electrified automotives. The lithium–oxygen battery is one candidate which could fulfil this increased demand due to the step change increase in specific energy it could potentially provide. However, several obstacles have now also become clear that hamper further progress [1]. During cycling of Li–O_2 batteries in non-aqueous electrolytes the oxygen reduction and oxidation evolution reactions (ORR and OER) take place in the pores of the carbon cathode during the discharge and charge respectively [2]. It has been shown that the ORR and OER result in the breakdown of not only the carbonate and ether based electrolytes [3–7] but also the salts such as $LiPF_6$, $LiB(CN)_4$, and LiBOB [6–8]. We have recently shown that the Kynar binder used for keeping the carbon cathode together also decomposes during the cycling of the Li–O_2 battery [7].

The mentioned studies [3–8] have focused solely on the degradation reactions occurring at the cathode of the battery with very little attention being placed on the stability of the Li anode or electrolytes in contact with Li anode in an oxygen atmosphere. Li metal is highly reactive, and in contact with non-aqueous liquids it is immediately covered by a passivation layer known as a solid electrolyte interphase (SEI) [9]. The SEI in alkyl carbonate based electrolytes has been widely attributed to the formation of lithium alkyl carbonate compounds ($ROCO_2Li$) and reduced electrolyte salts [10,11]. It has been shown that the thickness and the mass of the SEI on Li grows during cycling [12,13]. The chemistry and morphology has also been studied in the presence of trace amount of O_2 and H_2O in the electrolyte [14,15]. To the best of our knowledge all previous studies [10–16] of the SEI have focused on Li-ion batteries in a non-oxygen atmosphere.

* Corresponding author. Tel.: +46 18 471 3769; fax: +46 18 513548.
E-mail address: reza.younesi@kemi.uu.se (R. Younesi).

0378-7753/$ – see front matter © 2012 Elsevier B.V. All rights reserved.
http://dx.doi.org/10.1016/j.jpowsour.2012.10.011

In this short communication we seek to discuss for the first time the surface layer on the Li anode in a Li–O_2 cell and highlight the possible effects on the lithium deposition and stripping reaction. Here we present a detailed surface characterization of the Li anode used in Li–O_2 cells that have been cycled in 1 atm of dry oxygen with a 1 M $LiPF_6$ in PC electrolyte. This was performed using X-ray photoelectron spectroscopy (XPS) on anodes removed from Li–O_2 batteries, after a single discharge, a single discharge followed by a single charged, and from a battery which had been stored. We also examined the deposition and stripping of Li on copper using cyclic voltammetry (CV) in cells kept in an oxygen or argon atmosphere.

2. Experimental

The Li–O_2 cells were assembled in an Argon filled glove box using the Swagelok design with the following components; lithium foil as anode, 1 M $LiPF_6$ in PC as the electrolyte, Solupor separator, and porous cathodes. The porous cathodes were made by mixing Super P carbon (Lithium battery grade, Erachem Comilog) with α-MnO_2 nanowire catalyst and Kynar 2801 (Arkema) binder using propylene carbonate (PC) (Ferro, Purolyte) and acetone as plasticizer and solvent. The weight ratio of carbon:catalyst:binder:PC was equal to 11:19:15:55, and the weight ratio of acetone:carbon was equal to 60–70 to 1. The α-MnO_2 nanowire catalyst was synthesized as described in reference [17]. The slurries were kept under magnetic stirring for about 4 h and then cast into an aluminium mesh. The cathodes were dried at 120 °C overnight in a vacuum furnace within an argon filled glove box before using in batteries. The Swagelok™ design was modified such that an opening allowed oxygen to access through the cathode. The cells were kept in home-made air-tight containers with inlet and outlet valves for oxygen gas purging. The containers were filled with a continuous flow of dry oxygen for about 2 h before starting discharge. A current density of 70 mA g^{-1} (gram of carbon in the cathode) was applied using a Digatron BTS-600 with lower and higher cut-off voltages of 2.6 and 3.9 V vs. Li, respectively. The three batteries were then exposed to the following conditions: "Stored": kept in oxygen atmosphere for 2 days; "Discharged": first discharge to 2.6 V; "Charged": from freshly constructed discharged to 2.6 V and then charged to 3.9 V in constituting a single cycle. The current density of 70 mA g^{-1} was equal to ~0.025 mA cm^{-2} (area of the carbon electrode) for the "discharged" and "charged" cells, respectively. The discharge capacities of the cells were ~1.4 mAh cm^{-2}. The batteries were dismantled in an argon filled glove box and then, the Li anode was washed with a few drops of DMC prior to XPS characterization according to established procedures [18–20]. The effect of the washing procedure on the sample is still an open question for the experts in the XPS field. However, the general belief is that when an electrode is washed the XPS spectra originate from the SEI rather than from remaining salt and electrolyte solvent on the sample. Our several years' experience in XPS measurements indicates that results from the washed samples are usually more reproducible. This procedure is also commonly used also by other groups [18–20].

To avoid contact with air the Li anodes were transferred from the glove box to the XPS analysis chamber within 15 min using a special built air-tight argon filled chamber. The XPS measurements were performed on a commercial PHI 5500 spectrometer, using monochromatized Al Kα radiation (1487 eV) and an electron emission angle of 45°. The dimensions of the probed region were approximately 2 × 4 mm. All spectra were energy calibrated by the hydrocarbon peak at the binding energy of 285.0 eV.

Electrochemical deposition and stripping of lithium was investigated in 2 identical Swagelok cells, however, the porous cathode was replaced by a copper grid (200 mesh). The cells were then sealed in an argon atmosphere or stored under a continuous flow of dry oxygen. The cells were kept for 14 h before any electrochemical measurement. Electrochemical impedance spectroscopy was then performed using a Bio-Logic SP240 instrument in frequency range was from 100 kHz to 0.1 Hz and the amplitude was 20 mV p–p. This was followed by cyclic voltammetry from open circuit voltage (~3 V vs. Li/Li^+) to −0.5 V followed by 10 cycles in the range −0.5 V to 1 V at scan rate of 100 mV s^{-1}.

3. Results and discussion

Our interest in the Li anode–electrolyte interface was initiated when we visually observed a black layer on the Li surface after disassembling several cycled Li–O_2 cells. This black layer appeared to become thicker during battery cycling and was unlike anything we had observed on the Li anodes of Li-ion batteries which had been cycled with similar current densities in the absence of O_2. In the following study we investigated the surface composition of this layer in presence of O_2.

The XPS survey scan (Fig. 1) of the surface of the stored, discharged and charged Li anodes showed the presence of only expected elements, i.e. C, O, Li, F, and P. This shows that no contaminants are present on the sample, and especially the lack of N 1s signal confirms that no air exposures of the samples occurred prior to XPS measurements, i.e. during the cycling or XPS preparation. The survey scan shows the variation in relative surface concentrations of each element between the three samples, and these are also summarized in Table 1. The Li surface of the stored sample in oxygen atmosphere shows much larger concentrations of carbon and oxygen than previously reported for Li stored in the absence of oxygen (a detailed comparison is given in Table 2 [11]). The second column in Table 2 shows the relative element surface composition of the stored samples (the Li anode of a Li–O_2 battery kept under oxygen atmosphere for 2 days), estimated using XPS assuming a uniform distribution of elements. The third column in Table 2 shows the relative element surface composition of Li metals immersed in 1 M $LiPF_6$ in PC electrolyte in an oxygen free atmosphere obtained from a publication by D. Aurbach et al. [11]. We can conclude that the relative amounts C and O are higher in the Li–O_2 sample rather than in the O_2 free sample, while the relative amount of Li and F is reduced in the presence of oxygen. This suggests that

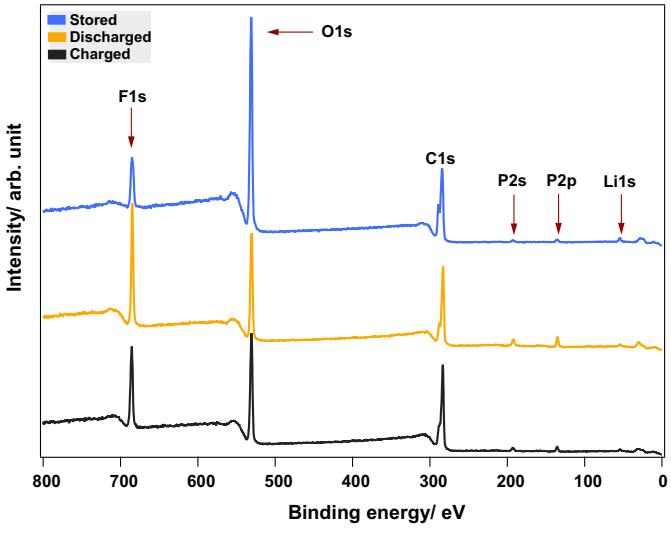

Fig. 1. Survey scan of Li anodes of the stored, discharged, and charged Li–O_2 cells containing 1 M $LiPF_6$ in PC.

Table 1
The relative element surface composition (at %) of the stored, discharged, and charged samples, estimated using XPS assuming a uniform distribution of elements.

Element	Stored	Discharged	Charged
C	41	45	50
O	34	22	23
Li	17	13	12
F	7	16	13
P	1	3.3	1.8

different products are formed on the surface of Li in the cell exposed to oxygen. This result should be anticipated when one considers the complex reactions (electrolyte breakdown) that occur during SEI formation on the surface and the high reactivity of oxygen and reduced oxygen species which will also be present. The higher amount of C present in the SEI layer seen in the oxygen cell compared to that in the non-oxygen cell suggests an increase in electrolyte breakdown products possibly resulting from reactions with or catalysed by the presence of oxygen.

After discharge and charge the surface composition (compared with stored) changes significantly with a reduction in the amount of Li and O (to similar concentrations in both cases) and an increase in the relative amounts of F and P. However, the relative amount of C in the surface layer increases from the discharged to the charged sample while the relative amounts of F and P decreases.

To quantitatively examine the chemical environments observed in this layer we de-convolved the high-resolution spectra. The results of this analysis together with the assignments of each peak for the surface layer in the stored, discharged and charged batteries are shown in Fig. 2. In Fig. 2 the same numbers of peaks at the same binding energies irrespective of the sample are visible in the C 1s, O 1s and Li 1s spectra. However, the intensity ratios of the peaks vary between the samples indicating a change in the relative surface concentration of the different compounds.

The binding energy positions of the de-convolved peaks and the relative amount of compounds are presented in Table 3. The peaks are assigned according to references [18–21]. The four peaks in the C 1s spectra indicate the presence of four different carbon bonding environments in the SEI layer of the stored sample (Fig. 2). The analysis shows almost similar amounts of ether and carbonate (11:8.6) suggesting the presence of lithium alkyl carbonates ($ROCO_2Li$). The discharged sample showed a decrease in the relative surface concentration of carbonates compared to that in the stored sample (C 1s spectra in Fig. 2). After charging the relative surface concentration of carbonates increased somewhat in the SEI layer whilst the ratio of carbonates to the ester/carboxylate species decreased indicating significant increase in the amount of ester/carboxylate species (Interestingly, this surface layer compositions is similar to which we have observed on the cathode of the discharged battery [6]). We also observed ether compounds that are not resulting from lithium alkyl carbonates (at least 11%–8.6% = 2.4% for the stored, 5.4% for the discharged, and 4% for the charged samples). These are assigned to the proposed decomposition products of carbonate based solvents and formation of poly(ethylene oxide) (PEO)-type or ROLi compounds [22]. The changes in the relative amount of these ether compounds and also the changes in the relative amount of hydrocarbons accounts for the changes which are seen in the surface concentration of carbon.

Table 2
The relative surface compositions (at %) of Li metal kept in contact with 1 M $LiPF_6$ in PC electrolyte in an O_2 atmosphere or in an O_2 free atmosphere.

Element	2 Days O_2 atm	3 Days[a] O_2 free
C	41	25.7
O	34	28.5
Li	17	36
F	7	9.7
P	1	0.2

[a] Obtained from reference [11].

The O 1s spectra of all the samples show two peaks at the binding energies of 532 and 533.5 eV. These two peaks represent carbonate/ester and ether compounds respectively. The O 1s spectra support the finding in the C1s spectra that the relative amount of carbonate/ester compounds together decreases compared to the relative amount of ether compounds from the stored to the discharged sample.

The F compounds found in the SEI layer of the stored sample were assigned to two types present in almost equal amounts (3% (LiF) + 4% ($LiPF_6$) = 7% (F)). The LiF peak originates from decomposition of the $LiPF_6$ salt [11,19]. This breakdown is verified from the P 2p spectra of the stored sample, which also shows two (spin-orbit split) peaks from P–F in $LiPF_6$ and P–O from decomposed $LiPF_6$. Whilst some of the $LiPF_6$ salt is decomposed, an almost equal amount is also trapped in the SEI layer. The relative surface concentration of P to F in the form of $LiPF_6$ (0.7:4) matches the ratio between P and F in the $LiPF_6$ molecule structure (1:6). Therefore, F and P are present as both $LiPF_6$ salt and decomposition products of the salt in the SEI of the stored Li.

After one discharge, the Li–F and P–O peaks almost disappear while the relative intensity of the $LiPF_6$ peak increases in both F 1s and P 2p spectra. This indicates that observed P and F species in the SEI layer for the discharged sample are from trapped rather than decomposed salt. We can also notice that the relative amounts of F and P on the surface of the sample increase (129% and 230% respectively). When we look at the charged sample we notice that again only $LiPF_6$ is present, however, the relative percentage of F and P (compared to the discharged) decreases by 19% and 45% respectively and the carbon contribution increases by 11%. This suggests that while after charge the observed species in the surface layer are similar as for the discharged a change in the abundance is observed. This combined with the changes seen in the C spectra suggests that the composition of the SEI layer changes as a function of the state of charge.

The F 1s spectrum for the charged sample surface shows another interesting feature which is a peak at 688 eV. This peak is absent in both the stored and discharged samples. The binding energy of this peak matches the binding energy of a C–F bond. It could be suggested that HF produced by hydrolyse of PF_6^-, reacts with the solvent, and consequently forms a CF_x containing compound [23]. However, the C–F bond peak appeared only in the charged sample not in the stored or discharged samples. We also see a similar high binding energy F 1s peak in the cathode in the discharge state [6]. Therefore, we believe that this high binding energy F 1s peak in the anode originates from a break-down of the Kynar binder and that the degradation products have been transported to the Li anode. A small peak at 293.8 eV in the C 1s spectra of the charged sample confirms formation of CF_3. In addition, we have observed similar behaviour (not presented in this study) from Kynar in Li–O_2 cells with a non-fluorinated salt, $LiClO_4$. Although it is known that Kynar binder decomposes on the cathode of a Li–O_2 battery forming LiF [7], it is a surprise to find it on the anode. It has been suggested that Kynar degrades to LiF through dehydrofluorination of PVDF by lithium superoxide (LiO_2) [24]. However, in this study we show that the Kynar binder component ($-CF_3$) is present in the SEI on the Li anode after charging the battery. Since this species is not found in any other component within the battery this implies that structure of the binder must have been unstable within the system. The chemical bonds in the binder have been broken and degradation products have been formed which are soluble or mobile fragments

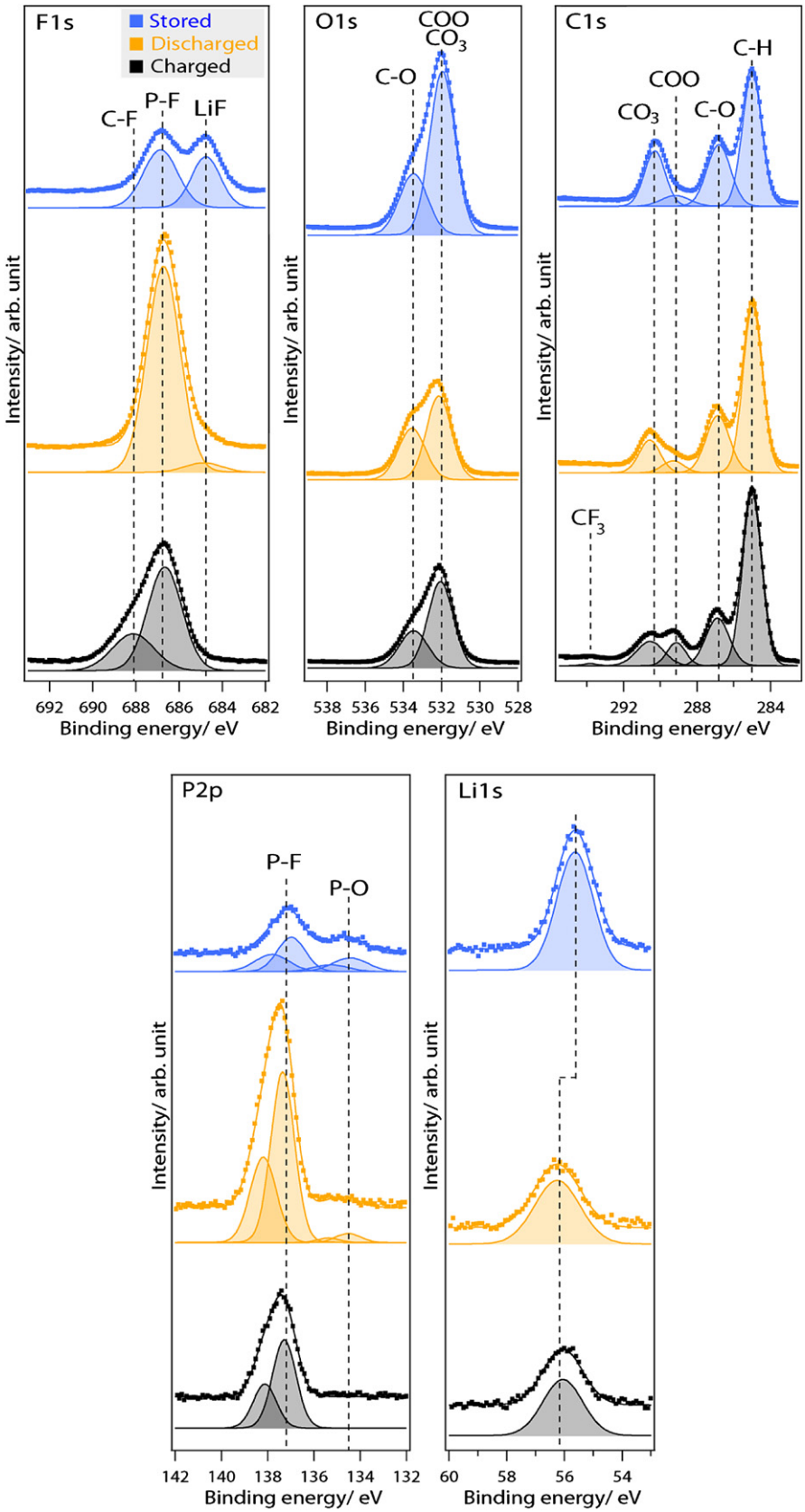

Fig. 2. F 1s, O 1s, C 1s, P 2p and Li 1s spectra of Li anode of the stored (top), discharged (middle) and charged (bottom), respectively, Li–O_2 batteries using 1 M $LiPF_6$ in PC as the electrolyte.

Table 3
A summary of XPS peaks assignments for the stored, discharged, and charged Li anode samples of Li–O_2 cells (Fig. 2).

	E_B/eV	Assignments	Concentration in the surface layer/at %		
			Stored sample	Discharged sample	Charged sample
C $1s^1$	285	Hydrocarbons	19	26	30
C $1s^2$	286.8	Ethers/alkoxides	11	11	10
C $1s^3$	289.1	Esters/ carboxylates	2.3	2.1	4
C $1s^4$	290.3	Carbonates	8.6	5.6	6
C $1s^5$	293.8	CF_3	–	–	0.3
O $1s^1$	532	Esters/ carboxylates/ carbonates	24	13	15
O $1s^2$	533.5	Ethers/alkoxides	10	8.8	7.6
F $1s^1$	684.8	LiF	3	0.8	–
F $1s^2$	686.8	$LiPF_6/Li_xPO_yF_z$	4	15	9.1
F $1s^3$	688.1	C–F	–	–	3.9
P $2p^1$	134.4	Phosphates	0.3	0.2	–
P $2p^2$	137.1	$LiPF_6$	0.7	3.1	1.8
Li $1s^1$	55.6–56.1		17	13	12

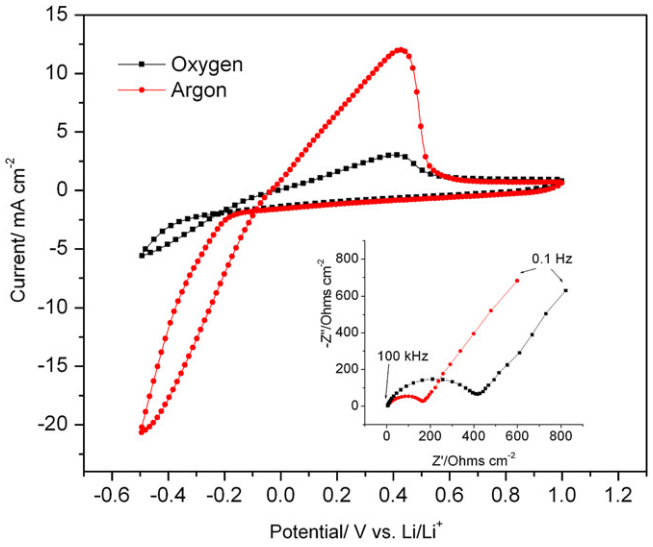

Fig. 3. Main: CV (100 mV s^{-1}) showing lithium deposition and stripping on Cu in the presence of oxygen and argon gas (shown is the 3rd cycle in both cases). Insert: AC impedance spectra recorded for both cells at 1 V vs. Li/Li^+ after 10 striping and deposition cycles.

and are transferred to the Li anode. Due to the large pores in the separator there is enough space for these fragments or dissolved species to pass through to the anode side. These results highlight that binder stability is key in the operation of the Li–O_2 battery since if unstable it can not only influence the cathode performance [25] but also the SEI formed on the Li anode.

The Li 1s spectra of the stored sample shows one peak at 55.6 eV, while that of the discharged and the charged samples show one peak at about 0.5 eV higher binding energy (56.1 eV). A change in the Li 1s peak is observed, however, it is difficult to assign it to specific compounds such as LiF, lithium alkyl carbonates etc as these all result in similar responses. It may have been expected that since we have dissolved oxygen and oxygen anions in solution near the lithium surface that Li_2O_2 may have been formed on the Li surface. However, neither the Li 1s or O 1s spectra indicates the presence of Li_2O_2 which would appear at binding energies of 531.5 and 54.6 in the O 1s and Li 1s spectra, respectively.

The XPS results can be summarized by:

- The presence of oxygen influences the surface elemental and species composition.
- Elemental and species composition in the surface layer change after discharging and again after charging.
- Decomposed binder is seen on the Li anode.

The SEI layer is also known to increase in thickness and mass during cycling from further electrolyte and salt decomposition and our results clearly indicate that the composition of this layer is also evolving.

As a preliminary investigation looking at the effect of this new layer on the electrochemical behaviour of the Li electrode we observed the deposition and stripping reaction of Li on a copper surface in PC electrolyte (recorded CV measurements are shown in Fig. 3, for additional information Figure S1 shows the first cycle measurement). In the case of the cell kept in argon the anticipated performance was observed [16]. The potential at which lithium plating begins is at around −0.2 V vs. Li/Li^+ and after reaching the negative potential limit at −0.5 V a nucleation loop is observed on the positive potential scan where lithium deposition continues until potentials greater than −0.1 V are reached. As the potential is increased further a positive current peak resulting from lithium stripping appears. When the cell was exposed to an oxygen atmosphere the same processes are observed, however, a significantly lower potential was required to initiate the plating of lithium metal and the plating reaction stops at a much lower potential on the positive potential scan. This indicates a significantly increased resistance in the cell which had been exposed to oxygen. To highlight this effect further we have additionally included Figure S2 in supplementary information. The AC impedance of both cells was measured after the cyclic voltammetry measurement was complete (Fig. 3 insert) at open circuit voltage (~1 V vs. Li). In both cases the impedance spectra shows a semi-circle shifted along the x axis followed by a ~60° spur. This is consistent with the results seen in a similar experimental set up [26–28] (In results not presented here, we also performed the impedance of both cells as constructed showing a similar semi circle diameter of ~150 Ω cm^{-2} for both cells). The equivalent circuit fitting model and fit results are included in supplementary information as Figures S3 and S4. The semi circle is a result of a parallel combination of a resistance and capacitance of the SEI layer formed at the interface of both the lithium and copper electrodes. An increase in SEI resistance (from 163 to 396 Ω cm^{-2}) for the cell stored in oxygen when compared to that stored in argon is observed. This increased resistance seen in the presence of oxygen after storage could either be a result of a thicker SEI layer or as a result of a reduced conductivity from the changing species observed in the layer. Further work is required to explain which explanation is correct.

4. Conclusions

To conclude we report a different and constantly evolving SEI layer on the Li anode in the Li–O_2 battery which significantly affects the cell performance. We believe that understanding the chemistry and morphology of this SEI layer is crucial component in developing a stable Li–O_2 battery. This area should be studied in much greater detail with special focus placed on new types of electrolytes to clarify how the surface chemistry of the Li is influenced. Also we must be aware that operation of both cathode and anode are connected (our data revealing the presence of decomposed binder on the lithium surface indicates cross-communication between the cathode and anode).

Acknowledgements

We would like to acknowledge Prof. Leif Nyholm and Dr. Fredrik Björefors, Uppsala University for useful discussions. We also acknowledge the Swedish Energy Agency (STEM), The Swedish Research Council (VR), StandUp for Energy and Storage within KIC InnoEnergy for financial support.

Appendix A. Supplementary information

Supplementary data related to this article can be found at http://dx.doi.org/10.1016/j.jpowsour.2012.10.011.

References

[1] P.G. Bruce, S.A. Freunberger, L.J. Hardwick, J.-M. Tarascon, Nat. Mater. 11 (2011) 19–29.
[2] K.M. Abraham, Z. Jiang, J. Electrochem. Soc. 143 (1996) 1–5.
[3] F. Mizuno, S. Nakanishi, Y. Kotani, S. Yokoishi, H. Iba, Electrochemistry 78 (2010) 403–405.
[4] W. Xu, K. Xu, V.V. Viswanathan, S. a. Towne, J.S. Hardy, J. Xiao, Z. Nie, D. Hu, D. Wang, J.-G. Zhang, J. Power Sources 196 (2011) 9631–9639.
[5] S.A. Freunberger, Y. Chen, N.E. Drewett, L.J. Hardwick, F. Bardé, P.G. Bruce, Angew. Chem. Int. Ed. 50 (2011) 8609–8613.
[6] R. Younesi, S. Urbonaitea, K. Edström, M. Hahlin, J. Phys. Chem. C 116 (2012) 20673–20680.
[7] R. Younesi, M. Hahlin, M. Treskow, J. Scheers, P. Johansson, K. Edstrom, J. Phys. Chem. C 116 (2012) 18597–18604.
[8] S. Hyoung Oh, T. Yim, E. Pomerantseva, L.F. Nazar, Electrochem. Solid State Lett. 14 (2011) A185.
[9] E. Peled, J. Electrochem. Soc. 126 (1979) 2047–2051.
[10] D. Aurbach, M.L. Daroux, P.W. Faguy, E. Yeager, J. Electrochem. Soc. 134 (1987) 1611–1620.
[11] D. Aurbach, I. Weissman, A. Schechter, H. Cohen, Langmuir 12 (1996) 3991–4007.
[12] K. Naoi, M. Mori, Y. Shinagawa, J. Electrochem. Soc. 143 (1996) 2517–2522.
[13] N. Takami, T. Ohsaki, K. Inada, J. Electrochem. Soc. 139 (1992) 1849–1854.
[14] K. Kanamura, H. Tamura, Z. Takehara, J. Electroanal. Chem. 333 (1992) 127–142.
[15] D. Aurbach, A. Zaban, Y. Gofer, Y.E. Ely, I. Weissman, O. Chusid, O. Abramson, J. Power Sources 54 (1995) 76–84.
[16] D. Pletcher, J.F. Rohan, A.G. Ritchie, Electrochim. Acta 39 (1994) 1369–1376.
[17] Y. Gao, Z. Wang, J. Wan, G. Zou, Y. Qian, J. Cryst. Growth 279 (2005) 415–419.
[18] S. Verdier, L. El Ouatani, R. Dedryvere, F. Bonhomme, P. Biensan, D. Gonbeau, J. Electrochem. Soc. 154 (2007) A1088–A1099.
[19] A.M. Andersson, K. Edstrom, J. Electrochem. Soc. 148 (2001) A1100–A1109.
[20] P. Verma, P. Maire, P. Novák, Electrochim. Acta 55 (2010) 6332–6341.
[21] A.M. Andersson, M. Herstedt, A.G. Bishop, K. Edström, Electrochim. Acta 47 (2002) 1885–1898.
[22] M. Herstedt, D.P. Abraham, J.B. Kerr, K. Edström, Electrochim. Acta 49 (2004) 5097–5110.
[23] Y.-C. Yen, S.-C. Chao, H.-C. Wu, N.-L. Wu, J. Electrochem. Soc. 156 (2009) A95–A102.
[24] R. Black, S.H. Oh, J.-H. Lee, T. Yim, B. Adams, L.F. Nazar, J. Am. Chem. Soc. 134 (2012) 2902–2905.
[25] S.R. Younesi, S. Urbonaite, F. Björefors, K. Edström, J. Power Sources 196 (2011) 9835–9838.
[26] A. Zaban, D. Aurbach, J. Power Sources 54 (1995) 289–295.
[27] H. Schranzhofer, J. Bugajski, H.J. Santner, C. Korepp, K.-C. Möller, J.O. Besenhard, M. Winter, W. Sitte, J. Power Sources 153 (2006) 391–395.
[28] L. Yang, C. Smith, C. Patrissi, C.R. Schumacher, B.L. Lucht, J. Power Sources 185 (2008) 1359–1366.